

Full-length article

Synergistic antitumoral activity and induction of apoptosis by novel pan Bcl-2 proteins inhibitor apogossypolone with adriamycin in human hepatocellular carcinoma

Jin-xia MI¹, Guang-feng WANG^{2,4}, Heng-bang WANG², Xiao-qing SUN¹, Xin-yan NI², Xiong-wen ZHANG², Jia-ming TANG¹, Da-jun YANG^{2,3}

¹Shanghai University of Traditional Chinese Medicine, Shanghai 201203, China; ²Ascenta (Shanghai) R&D Center, Shanghai 201203, China; ³Ascenta Therapeutics, Malvern, Pennsylvania, USA

Key words

apogossypolone; apoptosis; proto-oncogene protein bcl-2; combination drug therapy; adriamycin; hepatocellular carcinoma

⁴Correspondence to Dr Guang-feng WANG.
Phn 86-21-5132-0712.
Fax 86-21-5132-0612.
E-mail gwang@ascenta.com

Received 2008-06-07
Accepted 2008-09-18

doi: 10.1111/j.1745-7254.2008.00901.x

Abstract

Aim: To investigate the *in vitro* and *in vivo* activities and related mechanism of apogossypolone (ApoG2) alone or in combination with adriamycin (ADM) against human hepatocellular carcinoma (HCC). **Methods:** The IC₅₀ of ApoG2 *in vitro* was tested by WST assay, and the synergistic effect was analyzed using the CalcuSyn method. Cell apoptosis was determined using 4',6-diamidino-2-phenylindole staining and flow cytometric analysis. Western blotting was used to determine the expression of apoptosis-related proteins. *In vivo* activity was evaluated in the xenograft model in nude mice, and apoptosis in tumor tissues was determined by terminal deoxynucleotidyl transferase-mediated digoxigenin-dUTP nick-end labeling (TUNEL) assay. **Results:** The IC₅₀ of ApoG2 in HCC cells was 17.28–30.63 μmol/L. When ApoG2 was combined with ADM, increased cytotoxicity and apoptosis were observed in SMMC-7721 cells compared to treatment with ApoG2 alone. The Western blotting results indicated that the ApoG2 induced apoptosis in SMMC-7721 cells by downregulating anti-apoptotic proteins Bcl-2, Mcl-1, and Bcl-X_L, up-regulating pro-apoptotic protein Noxa, and promoting the activities of caspases-9 and -3. The tumor growth of xenograft SMMC-7721 was inhibited in nude mice when ApoG2 was administered orally without causing damage to the normal tissues. The *in vivo* study also indicated an increasing anti-tumoral effect when ApoG2 at 100 or 200 mg/kg dosages were used together with ADM at 5.5 mg/kg, with relative tumor proliferation rate (T/C) values of 0.456 and 0.323, respectively. Apoptosis induced *in vivo* by ApoG2 alone or combined with ADM was confirmed by TUNEL assay in tumor tissues. **Conclusion:** ApoG2 is a potential non-toxic target agent that induces apoptosis by upregulating Noxa, while inhibiting anti-apoptotic proteins and promoting the effect of chemotherapy agent ADM in HCC.

Introduction

Hepatocellular carcinoma (HCC) is the most common form of primary liver cancer and is the fifth most common cancer in the world, resulting in more than 660 000 deaths annually worldwide^[1,2]. Despite its rising incidence, the overall prognosis of HCC is poor, as systemic chemotherapy is of low efficacy^[3,4]. The most widely-used treatment is adriamycin (ADM), either

alone or in combination with other drugs. However, the response rate of ADM in a phase III clinical trials was only 10.5% when used alone and 20.9% for PIAF (cisplatin/interferon α-2b/ADM/fluorouracil) combination therapy^[5], but chemotherapy usually causes cytotoxicity with poor selection. Side-effects were frequently observed with each of the treatments. On the contrary, the newly-developed target therapies focus on the tumor-specific

proteins or kinases that are overexpressed in cancer cells or affect the development of tumors. Those agents have shown promising effects on liver cancer in clinical trials, such as the RAF/MAP kinase kinase (MEK)/extracellular signal-regulated protein kinase (ERK) pathway blocker Nexavar^[6], which is a multikinase inhibitor approved by the FDA for HCC therapy. Lifespan was prolonged by 44% in comparison with the placebo group according to the data of a phase III clinical trial^[7].

It is well-established that the overexpression of Bcl-2 family proteins plays an important role in tumor progression and drug resistance^[8-10], and is associated with unfavorable outcomes. The Bcl-2/Bcl-X_L protein has a Bcl-2 homology domain 3 (BH3)-binding groove that can be combined with many pro-apoptotic factors, such as Bad and Bak or BH3-only proteins, such as Bid, Bim, Noxa, and Puma and forms heterodimers, thereby inhibiting their function and inducing apoptosis. Targeting the BH3 domain of anti-apoptotic Bcl-2 members using non-peptide small-molecule inhibitors is a new and exciting therapeutic strategy^[11]. For example, ABT-737^[12], which has high affinity to Bcl-2 and Bcl-X_L, has shown potent inhibitory effects on the proliferation of tumor cells. Gossypol is another example of a potent inhibitor of Bcl-2 family proteins. It is a polyphenolic aldehyde occurring naturally in cottonseed. It has been used and extensively investigated as a male oral contraceptive agent and was recently discovered as a potent pan inhibitor of Bcl-2 family proteins^[13,14]. Gossypol has demonstrated beneficial anti-tumoral effect on a variety of cancer cells^[15-19]. Bcl-2-directed treatment targets cancer cells specifically overexpressing Bcl-2 proteins and is less toxic than traditional chemotherapy. Therefore, employing small molecules targeting Bcl-2 has become a popular approach for targeted cancer therapy.

To overcome the potential non-specific reactivity related to the 2 aldehyde groups in gossypol^[20], apogossypolone (ApoG2) was designed and synthesized, and 2 aldehyde groups of gossypol were completely removed (Figure 1). The K_i values of ApoG2 binding with Bcl-2, Mcl-1, and Bcl-X_L were 35, 25, and 660 nmol^[21], respectively. Studies

on ApoG2 for the treatment of pancreatic cancer, prostate cancer, leukemia, and lymphoma have been reported^[21-24]. The treatment of human pancreatic cell line BxPC-3 with curcumin sensitized ApoG2-induced cell killing. Bcl-X_L and Bcl-2 expression levels were downregulated, along with the inactivation of NF- κ B in combination with curcumin^[22]. In addition, a higher apoptotic index (94%) of ApoG2 was observed in combination with gemcitabine in BxPC-3 cells^[23]. An *in vivo* study showed that ApoG2 could significantly increase the lifespan of lymphoma-bearing SCID mice by at least 42%^[23]. Those results indicated that ApoG2 was a potential pan Bcl-2 family protein inhibitor, targeting Bcl-2, Mcl-1, and Bcl-X_L, and inducing apoptosis in cancer cells alone or in combination therapy.

As cancer cell-specific targets are not the only part of disease etiology, treatments combining targeted and conventional drugs may have a synergistic effect. In the present study, we investigated the *in vitro* and *in vivo* activities of ApoG2, as well as its activity in combination with chemotherapy agent ADM in HCC.

Materials and methods

Cells The human liver cancer cell lines SMMC-7721, Bel-7402, and QGY-7703 were purchased from Shanghai Institutes for Biological Sciences, Chinese Academy of Sciences (Shanghai, China). HepG2 was purchased from American Type Culture Collection (*Manassas, VA, USA*). All cells were cultured in RPMI-1640 (GIBCO, Gaithersburg, MD, USA) with 10% fetal bovine serum (GIBCO), 1% *L*-glutamine, 100 U/mL penicillin G, and 100 μ g/mL streptomycin. The cells were incubated at 37 °C in a humidified incubator with 5% CO₂.

Reagents ApoG2 were synthesized by Ascenta Therapeutics (Malvern, PA, USA). For the *in vivo* study, ApoG2 was suspended in 0.5% carboxymethylcellulose (CMC) solution and administered by oral gavage. ADM was purchased from Shanghai Richem International (Shanghai, China). For the intravenous treatment study, it was prepared in 0.9% sterile saline solution.

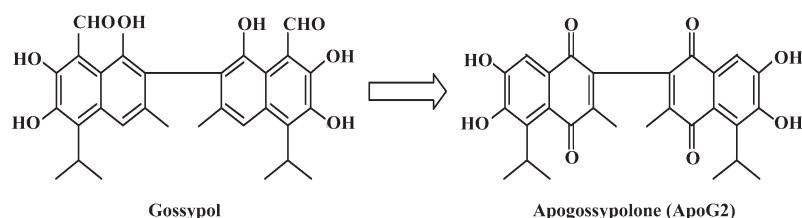


Figure 1. Structure modification of gossypol.

For the *in vitro* study, ApoG2 and ADM were dissolved in 100% DMSO and made to a 10 mmol/L store solution on the day of treatment. The working solution was prepared by dilution of the store solution with the culture medium.

Rabbit anti-Bcl-X_L (N_o 2762), p53 (N_o 9282), caspase-9 (N_o 9502), and caspase-3 (N_o 9665) antibodies were purchased from Cell Signaling Technology (Beverly, MA, USA). The rabbit anti-Bcl-2 (N_o 1017-1) antibody was purchased from Eptomics (Burlingame, CA, USA). The rabbit anti-Mcl-1 (N_o D1207) antibody was from Santa Cruz Biotechnology (Santa Cruz, CA, USA), The anti-Noxa (N_o D3601) antibody was purchased from Calbiochem (La Jolla, CA, USA), and peroxidase-conjugated goat antimouse immunoglobulin G (IgG; N_o 31430) and goat antirabbit IgG (N_o 31460) were purchased from Pierce Biotechnology (Rockford, IL, USA).

WST assay The inhibition of cell growth was determined by WST assay using cell counting kit-8 (CCK-8) from Dojindo Molecular Technologies (Kumamoto, Japan). The cells were seeded onto 96-well plates and treated with different concentrations of ApoG2 (0.1–80 μmol/L) alone for 72 h. The combinable effect of ApoG2 and ADM was assayed using the 2 agents separately (ApoG2 at 1.97–10 μmol/L or ADM at 0.11–0.6 μmol/L) or in combination and at a fixed drug dilution ratio. The cells were also treated for 72 h. Three repeat wells per treatment were required. After adding 10 μL CCK-8 to each well, the plates were incubated for 2 h. Absorbance at 450 nm was then measured using the Spectra Max 190 (Molecular Devices) microplate reader. Results were presented as the IC₅₀ of ApoG2, dose effect, and combination index (CI) values of ED₅₀, ED₇₀, and ED₉₀ for the combined treatment of ApoG2 and ADM.

The IC₅₀ was calculated with GraphPad Prism 4 software (Golden software, Golden, Colorado, USA). Drug interaction was evaluated by using CalcuSyn software (Biosoft, Ferguson, MO, USA). Drug combination studies were analyzed with the CI; CI values less than 1.00 were considered as showing synergetic effects.

4',6-Diamidino-2-phenylindole assays and flow cytometric analysis of apoptosis and cell cycle in cultured cells Cell apoptosis and the nuclei changes were estimated by 4',6-diamidino-2-phenylindole (DAPI) staining. The cells were seeded in 6-well plates and treated with ApoG2 (5, 10, or 15 μmol/L), ADM (1 μmol/L), and ApoG2 (10 μmol/L) in combination with ADM at (1 μmol/L). The cells in the control group were treated with the culture medium. The cells were collected 48 h after treatment and fixed with 4% formaldehyde; cell nuclei were stained

with DAPI (Sigma, St Louis, MO, USA). The stained cells were collected and the sections were made. The changes in the nuclei were observed under a fluorescent microscope with a 360 nm filter.

DNA contents were analyzed by flow cytometry. The cells were fixed by 70% ethanol at 4 °C for at least 1 h. After washing with phosphate-buffered solution (PBS), the cells were incubated in RNase A/PBS (100 mg/mL) at 37 °C for 30 min. Intracellular DNA was labeled with propidium iodide (PI) (50 mg/mL) and analyzed with a FACSCalibur fluorescent-activated cell sorter (FACS; Becton Dickinson, Franklin Lakes, NJ, USA). The cell cycle profile and apoptosis was obtained by analyzing 10000 cells.

Western blotting To determine changes in the protein levels, the cells were seeded onto 10 cm dishes and treated with ApoG2 at 5, 10, or 15 μmol/L, ADM at 1 μmol/L, and ApoG2 at 10 μmol/L in combination with ADM at 1 μmol/L. The control cells were treated with the culture medium. Floating and adherent cells were collected 48 h after treatment. For the P53 assay, the cells were collected 24 and 48 h after treatment. The cells were lysed using lysate buffer (Cell Signaling Technology, USA). The protein concentration of the supernatant was detected using the bicinchoninic Acid (BCA) protein assay kit (Beyotime Institute of Biotechnology, Haimen, China). The cell lysates were loaded to the 12% SDS gels and subsequently transferred to Hybond P membranes (GE Healthcare, USA). The first antibodies were incubated with the membranes at 4 °C overnight. The peroxidase-conjugated secondary antibodies were incubated with the membranes at room temperature for 2 h. Protein bonds were detected by ECL detection kit (GE Healthcare, USA).

Detecting the activation of caspases-9 and -3 The activities of caspases-9 and -3 of the cell lysates was measured using the caspase-9 and caspase-3 colorimetric assay kit (Nanjing KeyGen Biotechnology, Nanjing, China), according to the manufacturer's instructions. Alternatively, the cells were treated and collected as described in the Western blot assay. The protein concentration of the cell lysate was measured by BCA assay. The cell lysate was incubated with the chromophore-coupled substrates of caspases-9 and -3 at 37 °C for 4 h. The chromophore liberated from the substrate was measured using a plate reader at 405 nm. The activities were shown as the ratio of the optical density (OD) agent-treated sample/OD negative control sample.

Antitumoral effect of ApoG2 alone or in combination with ADM in animal models (nude mouse xenograft)

Female 6-week-old Balb/c *nu/nu* mice were purchased from Shanghai Laboratory Animal Center (Shanghai, China); 5×10^6 SMMC-7721 cells suspended in 0.2 mL PBS were inoculated sc to the right oxtor of each nude mice. Volumes of the tumor were estimated as $V=LW^2/2$, where L and W stand for tumor length and width, respectively. Mice with tumors at 50–150 mm³ were randomized into treatment groups (6 mice per group in the treatment groups, and 10 mice in the vehicle control group) and commenced treatment.

The mice were treated with ApoG2 at 100 and 200 mg/kg for 28 d by intragastric injection alone or in combination with ADM at 5.5 mg/kg once a week intravenously for 4 weeks. The positive control group was treated with ADM at 5.5 mg/kg once a week intravenously for 4 weeks. The vehicle control group was dosed ig daily with 0.5% CMC for 4 weeks. The individual relative tumor volume (RTV) was calculated as follows: $RTV=V_t/V_0$, where V_t is the volume on each day of measurement, and V_0 is the volume on the initial day of treatment. The therapeutic effect of the compound is expressed with the relative tumor proliferation rate (T/C). The calculation formula was: $T/C=\text{mean RTV of the treated group}/\text{mean RTV of the control group}$. Treatments producing >20% lethality and/or 20% net body weight loss were considered toxic.

Tissue microscopy In another pilot study, when the tumor size reached 150–200 mm³, 3 mice per group were treated with ApoG2 along (200 and 400 mg/kg, ig, daily) for 7 d, ADM at 10 mg/kg once intravenously on the first day, or ApoG2 in combination with ADM at 10 mg/kg. The vehicle control group was ig dosed daily with 0.5% CMC for 7 d. The mice were euthanized 2 h after the last treatment. Tumors and some tissues were removed from the animals and fixed in 10% formalin solution immediately. Tissues were paraffin embedded, and 0.5 μm -thick sections were prepared. The tumor, liver, lung, heart, kidney, spleen, and gastric tissues were stained with hematoxylin–eosin.

Terminal deoxynucleotidyl transferase-mediated digoxigenin-dUTP nick-end labeling assay To examine apoptosis in the specimens, sections were stained by terminal deoxynucleotidyl transferase dUTP nick end labeling (TUNEL) using the fluorescein FragEL DNA fragmentation detection kit (Calbiochem, USA), according to the manufacturer's instructions. Briefly, the slides were dewaxed in xylene and 70%–100% ethanol at room temperature as routine protocol. The slides were rinsed with 1×TBS and the entire specimen was incubated with 100 μL of 20 $\mu\text{g}/\text{mL}$ proteinase K at room temperature

for 20 min. The slides were rinsed with 1×TBS and the entire specimen were covered with 1 $\mu\text{g}/\mu\text{L}$ DNase I in 1×TBS/1 mmol/L MgSO₄. The slides were incubated at room temperature for 20 min. After washing with 1×TBS, the specimens were incubated with 100 μL of 1×terminal deoxynucleotidyl transferase (TdT) equilibration buffer at room temperature for 10–30 min. The 1×equilibration buffer was carefully blotted from the specimen and 60 μL TdT labeling reaction mixture was immediately applied onto each specimen. The slides were placed in a humidified chamber and incubated at 37 °C for 1–1.5 h. After washing with 1×TBS, the slides were mounted with a glass coverslip and the edges were sealed. The labeled nuclei in the slides were analyzed by using a standard fluorescent filter at 465–495 nm. Ten high-power fields were examined for each sample, and the number of cells stained positive in each field was determined. Values were then averaged to provide an apoptotic number for each tumor specimen, and an average of 3 tumors was determined for each tumor group.

Statistical analysis Statistical evaluation was performed using two-tailed *t*-test. *P*-values less than 0.05 were considered statistically significant.

Results

Evaluation of the combined growth inhibitory effects of ApoG2 and ADM in cultured human liver cancer cells

The *in vitro* cytotoxicity of ApoG2 on the 4 HCC cell lines were determined by WST assay (Figure 2). The 4 cell lines had a high expression level of Bcl-2 family proteins. The IC₅₀ value of ApoG2 for the SMMC-7721, Bel-7402, QGY-7703, and HepG2 cell lines were 17.28±4.71, 21.61±5.25, 17.36±4.30, and 30.63±3.83 $\mu\text{mol}/\text{L}$, respectively (Figure 2A). The most sensitive cell lines were SMMC-7721 and QGY-7703.

Increased cytotoxicity was observed when ApoG2 was used in combination with ADM in the HepG2, SMMC-7721, and QGY-7703 cell lines, calculated by the CalcuSyn method, but not in the Bel-7402 cell line. The data demonstrated that the CI plots of interactions between ApoG2 and ADM in HepG2, SMMC-7721, and QGY-7703 cells after 72 h treatment were less than 1.0 (Figure 2B, Table 1), which indicated synergy between two agents. As HepG2 has poor tumorigenicity in nude mice, and SMMC-7721 was the most sensitive cell line to ApoG2 in our studies and readily formed progressive tumors in nude mouse xenograft models, further detailed investigations were carried out in this cell line.

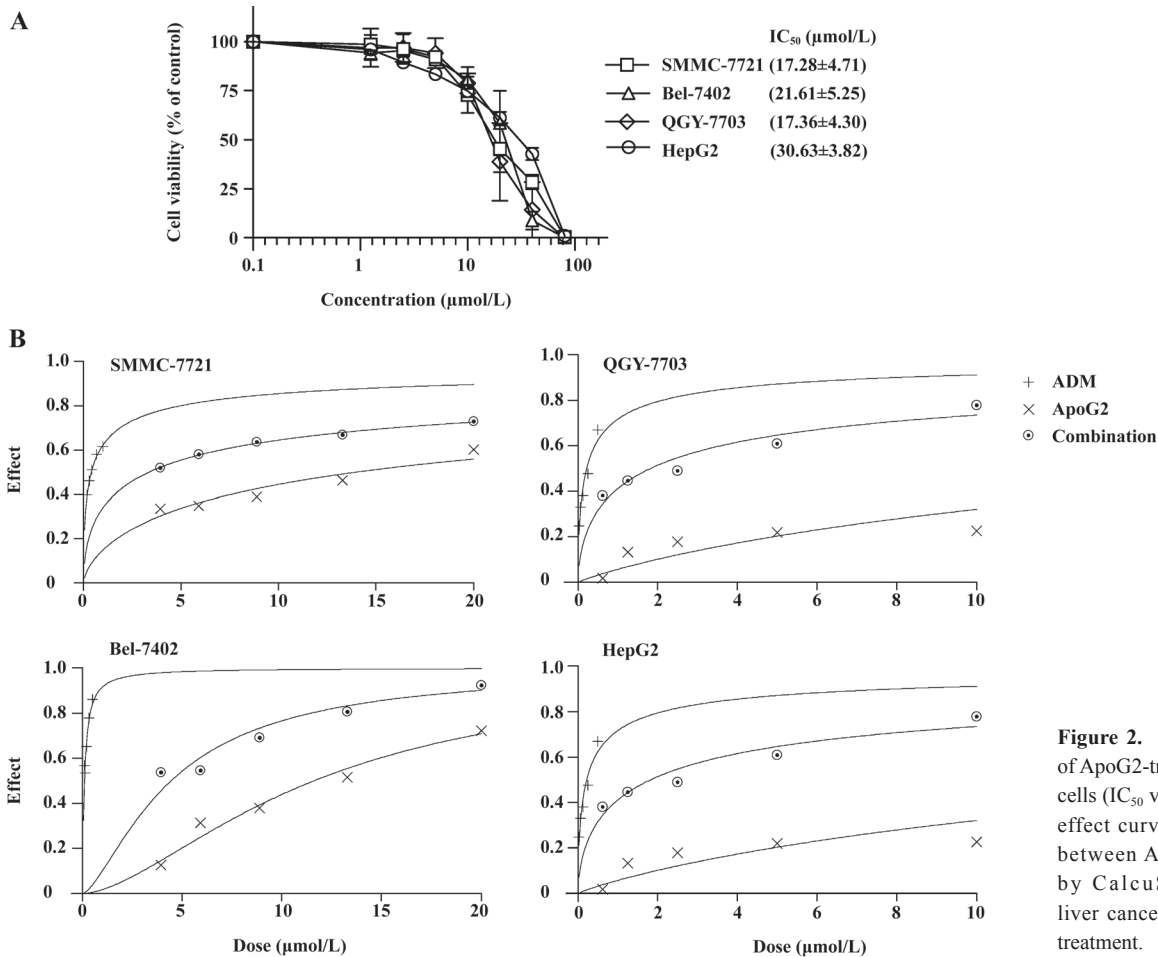


Figure 2. (A) Cell viability of ApoG2-treated liver cancer cells (IC₅₀ values). (B) Dose-effect curve of interactions between ApoG2 and ADM by CalcuSyn method in liver cancer cells after 72 h treatment.

Table 1. The CI values of interactions between ApoG2 and ADM by CalcuSyn method in four kinds of liver cancer cells after 72 h treatment.

Cells	Combination index values (CI)		
	ED ₅₀	ED ₇₅	ED ₉₀
SMMC-7721	0.657	0.763	0.911
QGY-7703	0.536	0.276	0.143
HepG2	0.499	0.578	0.712
Bel-7402	1.493	1.228	1.044

ApoG2 alone or in combination with ADM induced apoptosis of SMMC-7721 and influenced the expression of apoptosis-related proteins ApoG2 in combination with ADM resulted in increased apoptosis in SMMC-7721 cells. The results of the DAPI staining indicated that ApoG2 induced apoptosis alone or in combination with ADM (Figure 3A). The data of the FACS analysis demonstrated that ApoG2 at 5, 10, and 15 μmol/L increased the counting apoptosis rate by 3.87%, 12.92%, and 30.76%, respectively. The apoptosis rate for ADM at 1 μmol/L was 3.89%, and

an enhanced apoptosis rate of 18.67 % was detected for ApoG2 at 10 μmol/L with ADM at 1 μmol/L in the cultured cells (Figure 3C). The cell cycle analysis demonstrated that ApoG2 also induced cell arrest at the G₀/G₁ phase, whereas ADM caused S-phase arrest in SMMC-7721 cells, both alone and in combination, compared with 10 μmol/L ApoG2 (Figure 3B).

The expressions of anti-apoptotic proteins Bcl-2 and Mcl-1 were reduced by ApoG2 in a dose-dependent manner, and the expression of Bcl-X_L was completely inhibited by an even lower concentration of 5 μmol/L in this study. The BH3-only pro-apoptotic protein Noxa was increased by ApoG2 at 15 μmol/L. ApoG2 reduced full-form caspases-9 and -3, and the caspase activity assay indicated that the activities of caspases-9 and -3 increased in a dose-dependent manner. The results demonstrated that ApoG2 could induce apoptosis through the Bcl-2 pathway and activate a caspase cascade reaction (Figure 3C).

There appeared to be no difference in all of the protein expressions between 10 μmol/L ApoG2 alone and the

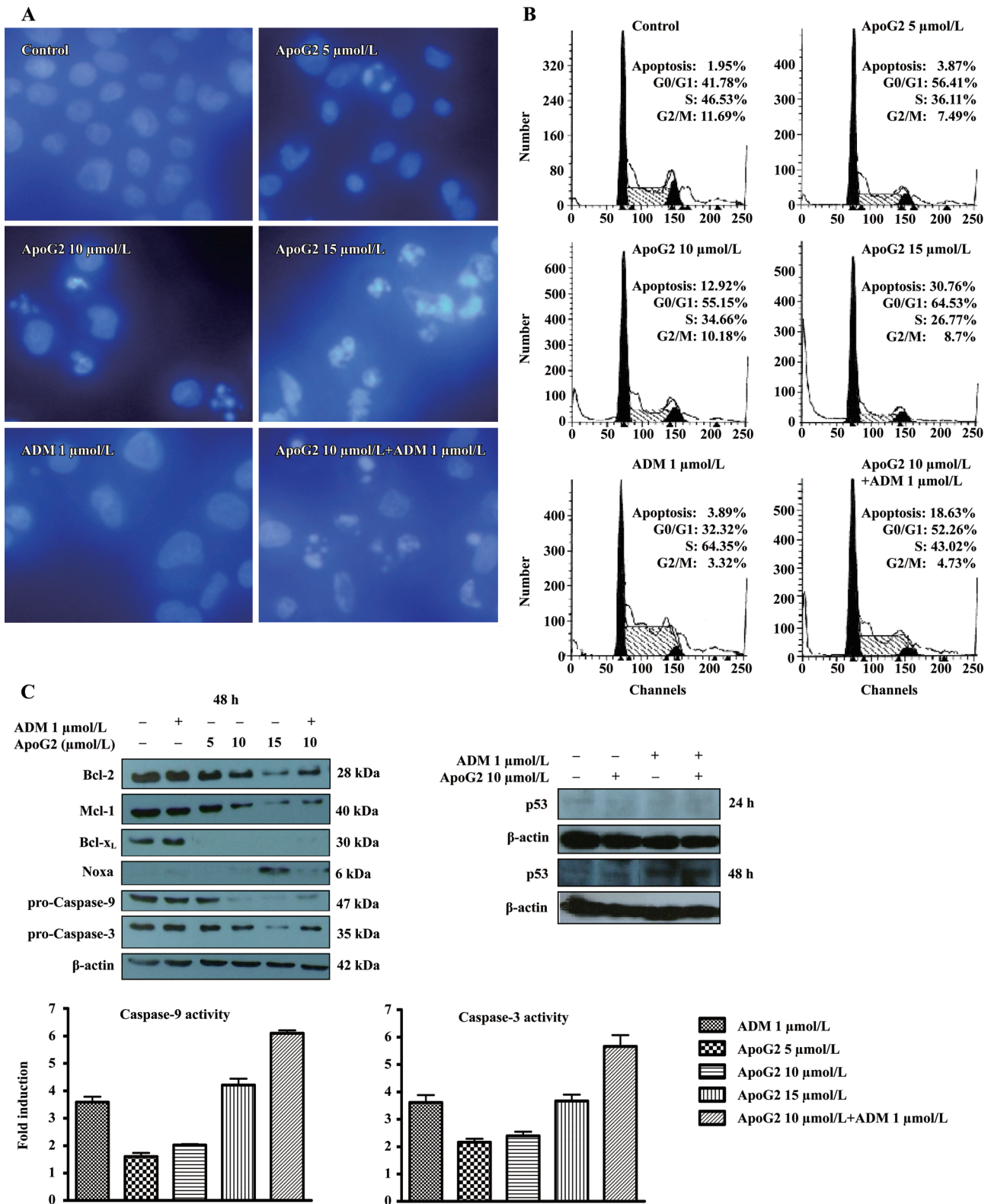


Figure 3. SMMC-7721 cells treated with ApoG2 single at 5, 10 or 15 μmol/L, ADM at 1 μmol/L or ApoG2 at 10 μmol/L in combination with ADM. (A) The condensed chromatin is seen as spot in the nucleus by DAPI staining after treatment for 48 h. (B) Cell cycle and apoptosis assay by FACS (PI staining) after treatment for 48 h. (C) Protein blotting after treatment for 24 h and 48 h and the caspase-9 and caspase-3 activity assay for 48 h.

combination of ApoG2 at 10 $\mu\text{mol/L}$ with ADM, according to the Western blot analysis. Although ADM alone did not affect the expression of Bcl-2 family members, it could promote the activities of caspases-9 and -3 and induce apoptosis for SMMC-7721. Enhanced activities of caspases-9 and -3 were observed in combination treatment. As p53 plays an important role in chemotherapy, further studies examining p53 should show that ADM increases the expression of p53 both alone and in combination with ApoG2 after treatment for 48 h (Figure 3C). The treatment of SMMC-7721 cells with concentrations up to 10 $\mu\text{mol/L}$ ApoG2 for 48 h did not produce significant changes in the levels of p53 in this assay.

Growth inhibition in the SMMC-7721 xenograft model In the liver cancer SMMC-7721 xenograft model, ApoG2 alone at a dose of 100 or 200 mg/kg (ig, once daily for 28 d) resulted in modest tumor growth inhibition with T/C values of 0.688 and 0.676, respectively. The T/C value for intravenous ADM at 5.5 mg/kg (once a week for 4 weeks) was 0.853, indicating limited or no antitumoral activity. An enhanced effect of ADM was observed when combined with ApoG2, with T/C values of 0.456 ($P<0.05$) and 0.323 ($P<0.01$) for 100 mg/kg ApoG2 with ADM or 200 mg/kg ApoG2 with ADM, respectively.

Significant body weight loss was not observed in the ApoG2-alone treatment groups compared with the control group during the experiment. However, ADM caused significant weight loss whether it was used alone or not ($P<0.05$), especially during the second and third weeks of treatment. Nevertheless, the weight changes were recovered after the cessation of treatment.

Figure 4C shows the damaged cells in combination therapy-treated tumor tissues. Compared with the control or single agent-dosing groups, there were spaces between the cells (cells were necrotic) and pyknotic nuclei in the slides of the tumor tissues of the combination groups. However, there were no significant lesions in the normal liver or other tissues, even with a high dose of ApoG2 (Figure 4D).

The results demonstrated that ApoG2 had low toxicity to normal tissues and demonstrated excellent therapeutic potential for human liver cancer either alone or in a combinable regimen.

Induction of apoptosis in tumor tissues The mice were treated with ApoG2 alone (200 or 400 mg/kg, ig, daily) for 7 d, or with ADM at 10 mg/kg once intravenously on the first day, or with ApoG2 in combination with ADM at 10 mg/kg. The vehicle control group was dosed ig daily with 0.5% CMC for 7 d. The mice were killed 2 h

after the last treatment. The apoptotic cells in the tumor sections were detected by TUNEL assay. In this assay, TdT bound to the exposed 3'-OH ends of DNA fragments generated in response to apoptotic signals and catalyzed the addition of fluorescein-labeled deoxynucleotides. The green fluorescent staining in the tumor sections represented apoptotic cells (Figure 5). The number of apoptotic cells in the ApoG2 alone group at 400 mg/kg was more than that of the ApoG2 alone group at 200 mg/kg. ApoG2 at 400 mg/kg with ADM at 10 mg/kg significantly induced more apoptotic cells in comparison with those treated with either ApoG2 or ADM alone in SMMC-7721 tumor tissues.

Discussion

ApoG2 is a potent, small molecule inhibitor of Bcl-2, Bcl-X_L, and Mcl-1 by binding to the BH3 binding pocket. The Bcl-2 family members all contain a BH3 domain, and it has been proposed that gossypol and its derivatives, acting as non-selective BH3 mimetic polygon, may bind to the BH3-binding pocket of various Bcl-2 family members. This binding activates Bak or Bax directly and promotes cell death, also simultaneously inhibiting anti-apoptotic members^[25]. Our study demonstrated that ApoG2 could dose dependently alter the expression of Bcl-2 family members, downregulating Bcl-2, Mcl-1 and Bcl-X_L, and up-regulating the expression of pro-apoptotic proteins, such as Noxa.

With the binding of ApoG2 to Bcl-2 family proteins, it would be expected that ApoG2 could lead to the activation of downstream apoptotic proteins. In the present study, we show that ApoG2 can activate caspase-9, which in turn activates caspase-3. Caspase-3 is one of the key executioners of apoptosis. Biochemical and genetic evidence indicates that Bcl-2 prevents apoptosis at the point of caspase-3 activation^[26]. Here, its changes corresponded with the results of induced apoptosis in SMMC-7721 cells.

These findings demonstrate that ApoG2 can activate the Bcl-2 apoptotic pathway *in vitro*. The exact mechanism of action of ApoG2 is still not clear. The proposed mechanisms would be that ApoG2 binds to Bcl-2 family members and its association interferes with BH3-only pro-apoptotic proteins, thus pro-apoptotic proteins participate in the apoptotic response. The results of the cell cycle assay also indicated that ApoG2 could induce cell cycle arrest at the G₀/G₁ phase in SMMC-7721 cells. Studies of (-)-gossypol show that it induces G₀/G₁ arrest in colon cancer and lymphoma cells^[27,28]. As a derivative of gossypol without two aldehyde groups, ApoG2 could

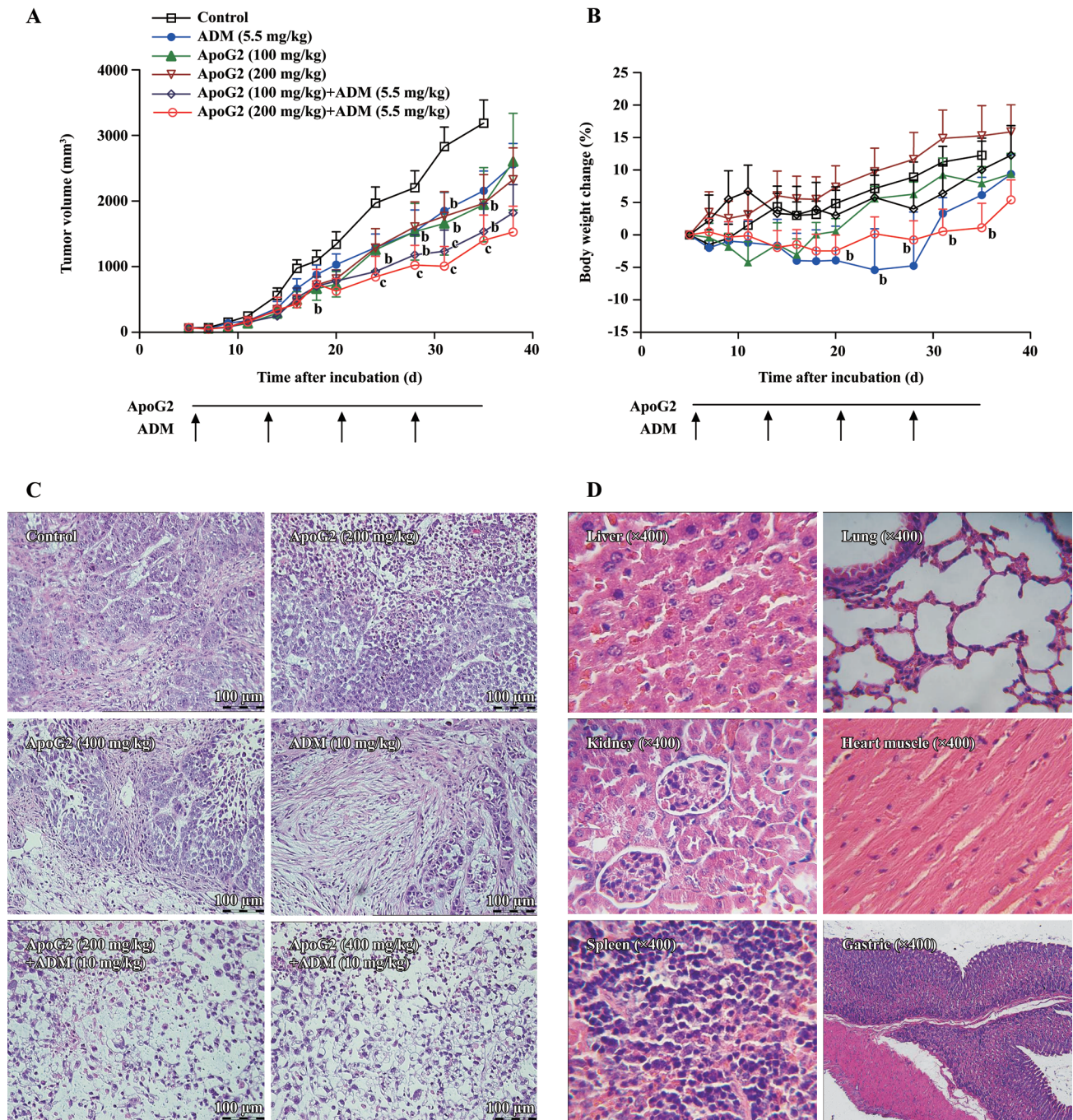


Figure 4. (A) Growth inhibition in xenograft SMMC-7721 model. Tumor growth curves show the mean tumor volume as a function of time. Tumor cells were inoculated into immunocompromised nude mice. After establishment of tumors, animals were treated po for 28 days on a daily schedule with ApoG2 and ADM iv once a week for 4 weeks at the concentration indicated. ^b*P*<0.05, ^c*P*<0.01, compared with control group. Tumor volumes in mice that received 100 or 200 mg/kg ApoG2 daily +ADM 5.5 mg/kg once a week were significantly smaller than tumor volumes in mice that received a vehicle control. This difference remained statistically significant from the 3rd to 4th weeks of the treatment. (B) Body weight change (%) of the tumor bearing mice during the treatment. There was no significant difference between the ApoG2 single treatment groups and the control group, *P*>0.05 compared with control group. But ADM (5.5 mg/kg) inhibited the growth of body weight in both single or combined groups, ^b*P*<0.05, compared with control group. (C) H&E stain of xenograft SMMC-7721 tumor tissues after 7 days treatment (×100). (D) H&E staining of normal tissues in xenograft SMMC-7721 model mice after 7 days treatment with ApoG2 400 mg/kg.

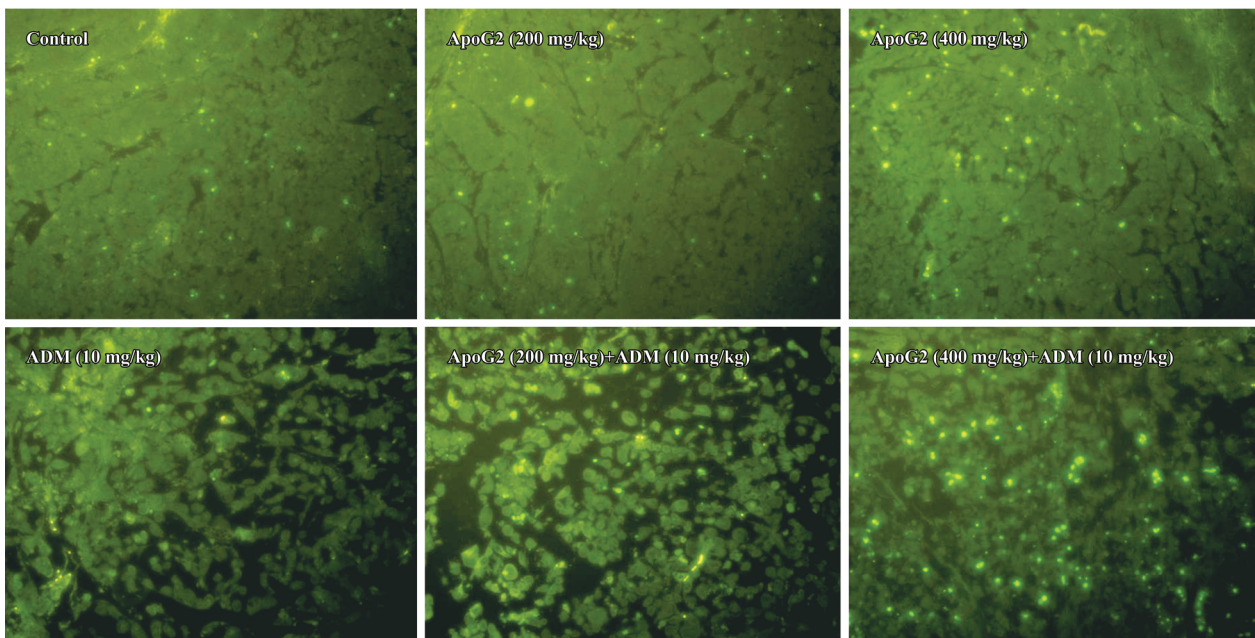
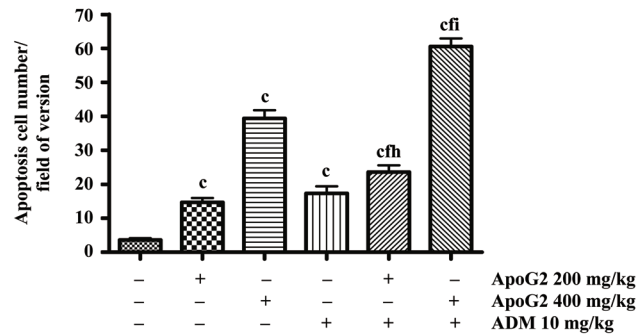


Figure 5. TUNEL assay results of SMMC-7721 xenograft tumor tissues after 7 days treatment, the bright fluorescence spots indicated the apoptosis cells. $n=10$. Mean \pm SEM. ^a $P<0.01$ compared with control group; ^f $P<0.01$ compared with ApoG2 single group; ^h $P<0.05$, ⁱ $P<0.01$ compared with ADM single group.

inhibit the proliferation of SMMC-7721 through cell cycle arrest and the induction of apoptosis.

The activation of P53, which promotes apoptosis of tumor cells, is considered to be a key mechanism of action of antitumoral drugs, including ADM^[29,30]. In this experiment, although ADM did not affect Bcl-2 family proteins of SMMC-7721, other studies on P53 showed that ADM could promote P53 expression. The results indicated that the promotion of P53 expression would be a possible cause for the induction of apoptosis by ADM in SMMC-7721 cells. ADM could inhibit biosynthesis of nucleic acid in tumor cells and cause cell toxicity in all the cell cycle phases. In our study, ADM at 1 μ mol/L induced S-phase arrest to SMMC-7721 cells. Nevertheless, based on the data presented in this study, apoptosis and cytotoxicity

induced by combination therapy of ApoG2 with ADM is more significant than with either agent alone.

The *in vivo* data found that the effect of ApoG2 alone was stronger than that of ADM alone, and that ApoG2 alone at an oral dose of 100 or 200 mg/kg, once daily for 28 d, resulted in modest tumor growth inhibition and T/C values of 0.688 and 0.676, respectively, in the liver cancer SMMC-7721 xenograft model. The T/C value for intravenous ADM at 5.5 mg/kg (once a week for 4 weeks) was 0.853. More importantly, there was no body weight loss in the animals treated with ApoG2 with all doses, indicating no toxicity to the animals at the dosages administered. The maximal tolerated dose (MTD) of ApoG2 in the mice by oral gavage was more than 2000 mg/kg in our separate studies. Furthermore,

histopathological examinations indicated that no lesions were found in the normal tissues of major organs in mice after continuing treatment with ApoG2 at 400 mg/kg for 7 d. The combination treatment did not result in greater toxicity to the animals. When combined with ADM, an enhanced effect of ApoG2 was observed, with T/C values of 0.456 ($P < 0.005$) and 0.323 ($P < 0.001$) for the 100 mg/kg plus ADM and 200 mg/kg plus ADM groups, respectively. These results indicate that ApoG2 would be a safe and effective agent for anti-liver cancer therapy either alone or in combination therapy.

In summary, the data demonstrated that ApoG2 can promote apoptosis through the Bcl-2 pathway by upregulating the BH3-only pro-apoptotic protein Noxa and downregulating Bcl-2, Mcl-1, and Bcl-X_L in SMMC-7721 cells. ApoG2 could have great therapeutic potential as an effective new therapy for HCC when used with traditional chemotherapy ADM.

Author contribution

Guang-feng WANG and Xiong-wen ZHANG designed research; Jin-xia MI, heng-bang WANG, Xiao-qin SUN and Xin-yan NI performed research; Ascenta(shanghai) R&D Center contributed all analytical tools and reagents; Guang-feng WANG, Da-jun YANG, Xiong-wen ZHANG and Jia-ming TANG analyzed data; Jin-xia MI and Guang-feng WANG wrote the paper.

References

- Llovet JM, Burroughs A, Bruix J. Hepatocellular carcinoma. *Lancet* 2003; 362: 1907–17.
- World Health Organization. Media centre factsheets. Available from URL: www.who.int/mediacentre/factsheets/fs297/en
- Simonetti RG, Liberati A, Angiolini C, Pagliaro L. Treatment of hepatocellular carcinoma: a systematic review of randomized controlled trials. *Ann Oncol* 1997; 7: 387–96.
- Simonetti RG, Liberati A, Angiolini C, Pagliaro L. Treatment of hepatocellular carcinoma: a systematic review of randomized controlled trials. *Ann Oncol* 1997; 8: 117–36.
- Yeo W, Mok TS, Zee B, Leung TW, Lai PB, Lau WY, *et al*. A randomized phase III study of doxorubicin versus cisplatin/interferon alpha-2b/doxorubicin/fluorouracil (PIAF) combination chemotherapy for unresectable hepatocellular carcinoma. *J Natl Cancer Inst* 2005; 97: 1532–8.
- Liu L, Cao YC, Chen C, Zhang XM, McNabola A, Wilkie D, *et al*. Sorafenib blocks the RAF/MEK/ERK pathway, inhibits tumor angiogenesis, and induces tumor cell apoptosis in hepatocellular carcinoma model PLC/PRF/5. *Cancer Res* 2006; 66: 11 851–8.
- Llovet J, Ricci S, Mazzaferro V, Hilgard P, Raoul J, Zeuzem S, *et al*. Randomized phase III trial of sorafenib versus placebo in patients with advanced hepatocellular carcinoma (HCC). *J Clin Oncol* 2007 ASCO Annual Meeting Proceedings (Post-Meeting Edition); 2007; 25 Suppl: LBA1.
- Lacronique V, Minon A, Fabre M, Viollet B, Rouquet N, Molina T, *et al*. Bcl-2 protects from lethal hepatic apoptosis induced by an anti-Fas antibody in mice. *Nat Med* 1996; 2: 80–6.
- Chuna EY, Lee KY. Bcl-2 and Bcl-x_L are important for the induction of paclitaxel resistance in human hepatocellular carcinoma cells. *Biochem Biophys Res Commun* 2004; 315: 771–9.
- Takahashi M, Saito H, Atsukawa K, Ebinuma H, Okuyama T, Ishii H. Bcl-2 prevents doxorubicin-induced apoptosis of human liver cancer cells. *Hepatol Res* 2003; 25: 192–201.
- Wang S, Yang D, Lippman ME. Targeting Bcl-2 and Bcl-X_L with nonpeptidic small-molecule antagonists. *Semin Oncol* 2003; 30: 133–42.
- Oltersdorf T, Elmore SW, Shoemaker AR, Armstrong RC, Augeri DJ, Belli BA, *et al*. An inhibitor of Bcl-2 family proteins induces regression of solid tumours. *Nature* 2005; 435: 677–81.
- Zhai D, Jin C, Satterthwait AC, Reed JC. Comparison of chemical inhibitors of antiapoptotic Bcl-2-family proteins. *Cell Death Differ* 2006; 13: 1419–21.
- Oliver CL, Bauer JA, Wolter KG, Ubell ML, Narayan A, O'Connell KM, *et al*. *In vitro* effects of the BH3 mimetic, (-)-gossypol, on head and neck squamous cell carcinoma cells. *Clin Cancer Res* 2004; 10: 7757–63.
- Lei XB, Chen YY, Du GH, Yu WY, Wang XH, Qu H, *et al*. Gossypol induces Bax/Bak-independent activation of apoptosis and cytochrome *c* release via a conformational change in Bcl-2. *FASEB* 2006; 20: E1510–9.
- Mohammad RM, Wang SM, Aboukameel A, Chen B, Wu XH, Chen JY, *et al*. Preclinical studies of a nonpeptidic small-molecule inhibitor of Bcl-2 and Bcl-X_L [(-)-gossypol] against diffuse large cell lymphoma. *Mol Cancer Ther* 2005; 4: 13–21.
- Bauer JA, Trask DK, Kumar B, Los G, Castro J, Lee J S, *et al*. Reversal of cisplatin resistance with a BH3 mimetic, (-)-gossypol, in head and neck cancer cells: role of wild-type p53 and Bcl-xL. *Mol Cancer Ther* 2005; 4: 1096–104.
- Huang YW, Wang LS, Chang HL, Ye WP, Dowd MK, Wan PJ, *et al*. Molecular mechanisms of (-)-gossypol-induced apoptosis in human prostate cancer cells. *Anticancer Res* 2006; 26: 1925–34.
- Wolter KG, Wang SJ, Henson BS, Wang SM, Griffith KA, Kumary B, *et al*. (-)-Gossypol inhibits growth and promotes apoptosis of human head and neck squamous cell carcinoma *in vivo*. *Neoplasia* 2006; 8: 163–72.
- Stein RC, Joseph AE, Matlin SA, Cunningham DC, Ford HT, Coombes RC. A preliminary clinical study of gossypol in advanced human cancer. *Cancer Chemother Pharmacol* 1992; 30: 480–2.
- Zhang Y, Ling X, Zhang XW, Lin YQ, Min P, Stoudemire J, *et al*. A novel pan inhibitor of Bcl-2 and Mcl-1 apogossypolone (ApoG2) with superior stability and improved activity against human leukemia and lymphoma cells. *Proceedings of 98th AACR Annual Meeting*; 14–18 Apr 2007; Los Angeles, CA, USA.
- Thoutreddy S, Mohammad RM, Ali S, Wang SM, Sarkar H. Curcumin sensitizes pancreatic cancer cells to ApoG2 induced killing. *Pancreas* 2006; 33: 502. [Abstract]
- Arnold AA, Aboukameel A, Chen JY, Yang DJ, Wang SM, Al-Katib A, *et al*. Preclinical studies of apogossypolone: a new nonpeptidic pan small-molecule inhibitor of Bcl-2, Bcl-X_L and Mcl-1 proteins in follicular small cleaved cell lymphoma model. *Mol Cancer* 2008; 7: 20.

- 24 Choi M, Wang SM, Banerjee S, Sarkar F, Mohammad R. Bcl-2 and Bcl-xL targeted therapy inhibits growth of pancreatic cancer cells. 2006 Gastrointestinal Cancers Symposium; 26–28 Jan 2006; San Francisco, CA, USA.
- 25 Oliver CL, Miranda MB, Shangary S, Land S, Wang S, Johnson DE. (-)-Gossypol acts directly on the mitochondria to overcome Bcl-2- and Bcl-X(L)-mediated apoptosis resistance. *Mol Cancer Ther* 2005; 4: 23–31.
- 26 Li P, Nijhawan D, Budihardjo I, Srinivasula SM, Ahmad M, Alnemri ES, *et al*. Cytochrome c and dATP-dependent formation of Apaf-1/caspase-9 complex initiates an apoptotic protease cascade. *Cell* 1997; 91: 479–89.
- 27 Zhang M, Liu H, Guo R, Ling Y, Wu X, Li B, *et al*. Molecular mechanism of gossypol-induced cell growth inhibition and cell death of HT-29 human colon carcinoma cells. *Biochem Pharmacol* 2003; 66: 93–103.
- 28 Li ZM, Jiang WQ, Zhu ZY, Zhu XF, Zhou JM, Liu ZC, *et al*. Synergistic cytotoxicity of Bcl-xL inhibitor, gossypol and chemotherapeutic agents in non-Hodgkin's lymphoma cells. *Cancer Biol Ther* 2008; 7: 51–60.
- 29 Wang S, Konorev EA, Kotamraju S, Joseph J, Kalivendi S, Kalyanaraman B. Doxorubicin induces apoptosis in normal and tumor cells via distinctly different mechanisms. Intermediacy of H₂O₂- and p53-dependent pathways. *J Biol Chem* 2004; 279: 25 535–43.
- 30 Wei S, Liu G, Yang J, Sheng W, Wu H. The experimental research of the induction of apoptosis in human hepatocellular cancer cell line SMMC-7721 by pharmorubicin. *Jiangsu Med J* 2002; 28: 23–5.